JOURNAL OF THERMOPHYSICS AND HEAT TRANSFER
Vol. 20, No. 2, April–June 2006

Analytical Model for Thermal Performance Analysis of Enclosure Heated by Aligned Thermosyphons

Fernando H. Milanez* and Marcia B. H. Mantelli†
Federal University of Santa Catarina, 88040-900 Florianopolis, SC, Brazil

An analytical model is developed to analyze the thermal performance of a rectangular enclosure heated by two-phase thermosyphons. The model is used to predict temperatures and thermal resistances between the elements of the enclosure based on experimental data obtained from an actual enclosure heated with a total heat input of 1280 W from room temperature and up to a maximum temperature of 330°C. The rms differences between the model and the experimental data vary between 3.4 and 7.6°C. Thermal joint resistances that are difficult to predict are evaluated indirectly by means of the proposed model. The model is also used to estimate the relative importance of the three heat-transfer modes inside the enclosure. The results show that, given the very isothermal characteristic of the air inside the enclosure, which does not lead to effective natural convection heat transfer, most of the heat inside the enclosure is transported by radiation and by conduction. Also, the usual approach of riveted joints employed in domestic ovens is shown to be thermally inefficient.

Nomenclature

A	=	surface area, m^2
c	=	specific heat, $J/kg \cdot K$
e	=	thickness, m
F	=	view factor
h	=	convection heat-transfer coefficient, $W/m^2 \cdot K$
k	=	thermal conductivity, $W/m \cdot K$
m	=	mass, kg
N	=	number of thermosyphons
q	=	heat-transfer rate, W
R_c	=	thermal contact resistance between the thermosyphon condenser and the fin, K/W
T	=	temperature, K
t	=	time, s
ε	=	surface emissivity
σ	=	5.67×10^{-8} W/m^2K^4 (Stefan–Boltzmann constant)

Subscripts

air	=	air inside the enclosure
amb	=	external ambient
c	=	thermosyphon condenser
cav	=	enclosure
cond	=	conduction
conv	=	convection
e	=	thermosyphon evaporator
ext	=	external
e.walls	=	external walls
f	=	working fluid
fin	=	fin
ins	=	insulation blanket
int	=	internal
i.walls	=	external walls
p	=	constant pressure
rad	=	radiation
t	=	thermosyphon
v	=	constant volume

Received 4 November 2004; presented as Paper 2005-0382 at the AIAA 43rd Aerospace Sciences Meeting and Exhibit, Reno, NV, 10–13 January 2005; revision received 22 March 2005; accepted for publication 26 March 2005.

*Research Engineer, Department of Mechanical Engineering, Satellite Thermal Control Group; milanez@labsolar.ufsc.br.

†Professor, Department of Mechanical Engineering, Satellite Thermal Control Group; marcia@labsolar.ufsc.br.

Introduction

TWO-PHASE thermosyphons are high-efficiency heat-transfer devices. Various thermosyphon configurations have been developed over the last decades for different applications, including high-performance heat exchangers for nuclear energy and petroleum refinery industries, solar-energy absorbers, to name a few. Faghri[1] and Peterson,[2] among others, present reviews on the heat pipe and two-phase thermosyphon technology and applications. The thermosyphon thermal resistance is very low because during liquid–vapor phase change there is no temperature variation. The thermal resistance of the thermosyphon is basically determined by the thermal resistances of conduction through the tube walls and by the thermal resistances of vaporization and condensation of the working fluid, which are generally very small. Apart from featuring a very low thermal resistance, another important characteristic of two-phase thermosyphons is a very uniform temperature distribution in the condenser section when the external heat-transfer coefficient is small. Recently, Mantelli and coworkers[3–6] have successfully applied two-phase thermosyphons to isothermalize enclosures, such as bakery ovens. The objective of this work is to develop an analytical model to predict the thermal performance of this type of enclosure. A lumped temperature methodology is employed to compute the temperature variations with time of each component of the system and the thermal interaction among the components.

Problem Statement and Geometry

The geometry of the enclosure under study is presented in Fig. 1. It is composed basically of two mild steel sheets, which constitute the top and bottom walls and two aluminum sheets (side walls) attached to each other by means of riveted joints (Fig. 1a). The sheets are assembled in the form of a rectangular enclosure (Fig. 1b) with dimensions $0.38 \times 0.48 \times 0.61$ m. Eight thermosyphons are attached internally to side walls of the enclosure (Fig. 1c), so that the side walls act as fins, helping to remove the heat from the thermosyphon condensers. The thermosyphon evaporators are tilted at 45 deg and are located inside a combustion chamber below the enclosure. Two metal sheets are riveted at the front and at the back of the enclosure (Fig. 1d). An insulation blanket made of glass wool is wrapped around the enclosure sheets and thermosyphons (Fig. 1e). Mild steel sheets are placed externally to protect the insulation blanket (Fig. 1f). A glass wool blanket is used to insulate the enclosure back wall (Fig. 1g). The front door, made of glass wool sandwiched by metal

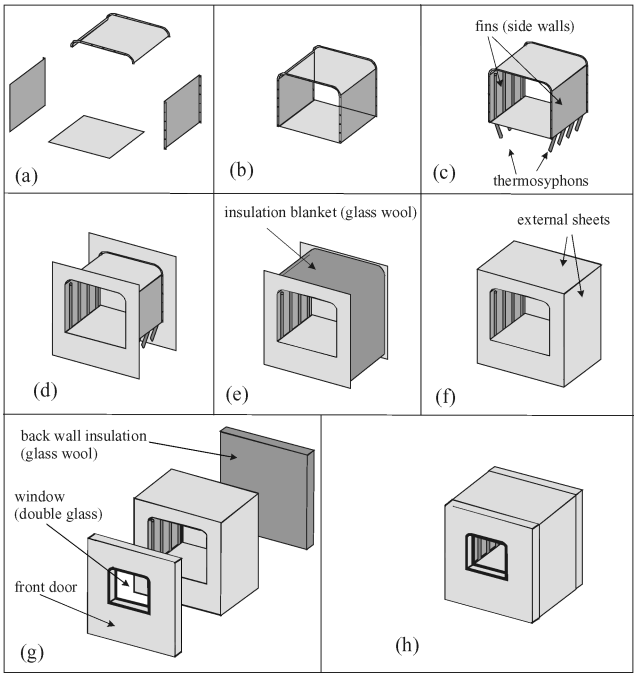

Fig. 1 Enclosure geometry.

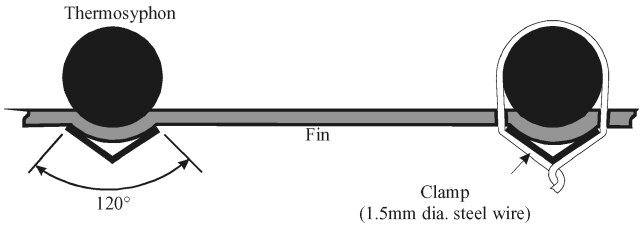

Fig. 2 Details of the thermosyphons/fin attachment.

sheets, completes the enclosure (Fig. 1g). At the center of the front door, there is a double glass window for inspection.

Eight 12.7 mm outer diameter and 10.2 mm inner diameter stainless-steel thermosyphons are used. The working fluid is distillated water. The condenser section of the thermosyphons is 270 mm long and is located inside the enclosure, attached to the side walls. The thermosyphons have no adiabatic zone, and the evaporators are 90 mm long. The nominal filling ratio is 100% of the evaporator volume. A gas burner is placed below each row of evaporators. The evaporators and the burner are confined in a combustion chamber, completely separated from the enclosure. The number of thermosyphons was determined based on the results of previous works.[3–5] The geometry of the enclosure and the heat-flux density in the evaporator section of the thermosyphons used in this study are approximately the same as in the bakery oven studied earlier. The spacing between the thermosyphons was determined by simply dividing the length of the enclosure (0.48 m) by four, which is half the total number of thermosyphons.

The details of the thermosyphon/fin attachment are shown in Fig. 2. The condenser fin was deformed to accommodate $\frac{1}{3}$ the circumferential area of the thermosyphon along the entire length of the condenser. The fin is sandwiched between the thermosyphon and a steel angle. A steel wire clamp is used to squeeze the fin against the thermosyphon. The function of the steel angle is to distribute the contact pressure evenly over the interface, minimizing the occurrence of gaps where there is no effective contact, which would lead to a larger thermal resistance at the joint between the thermosyphon and the fin. An aluminum tape is placed between thermosyphon and the fin. Under compression, the aluminum tape deforms easily, helping to fill the gaps between the thermosyphon and the fin and minimizing the overall thermal resistances of these interfaces.

The objective of this work is to develop a theoretical model that can be used to analyze the thermal performance of the enclosure. By "analysis of thermal performance," one means three main aspects: 1) estimation of the temperature variations of the enclosure components with time for a given initial condition and for a given heat power input; 2) estimation of the thermal resistances between the metal sheets that constitute the fins and the enclosure internal and external walls, and the thermal resistance between the thermosyphon and the fin; and 3) estimation of the percentage of each heat-transfer mode (conduction, convection, and radiation) among the enclosure elements.

Enclosure Theoretical Model

The physical model adopted for the heat-transfer path is described now. The hot exhaust gases inside the combustion chamber heat the thermosyphon evaporators by radiation and convection. The thermosyphon transport the heat from the evaporator end to the condenser end. From the condensers, heat is transferred by radiation to the enclosure internal walls, by convection to the air inside the enclosure and by conduction and radiation to the fins. The fins lose heat by radiation to the enclosure internal walls, convection to the air, and conduction to the insulation blanket and to the enclosure internal walls through the riveted joints. The air receives heat by convection only because, in the range of temperatures of interest (below 330°C), it is transparent to thermal radiation. According to the procedure described by Incropera and De Witt,[7] only water vapor and CO_2 participate in radiation heat exchanges. The other gases present in the air are transparent to thermal radiation. The contribution of vapor water and CO_2 was estimated to be approximately 5%, which is the value of the effective emissivity of the air inside the enclosure. Because this parcel is small, the air is assumed to be transparent to thermal radiation. Heat reaches the air by convection coming from the fins and from the condensers. The air transports heat to the enclosure internal walls (back wall, bottom wall, top wall, and door) by means of convection. The enclosure internal walls receive heat by radiation (from the thermosyphons and the fins), by conduction (from the fins through the riveted joints), and by convection (from the air). The internal walls (door, back, bottom, and top) transfer heat by conduction to the insulation blanket and also to the enclosure external walls through "thermal short circuits" between the internal and the external walls. These short circuits are thermal paths between the internal and external walls other than conduction through the insulation blanket, such as riveted joints that attach the enclosure internal walls to the enclosure external walls, radiation heat losses through the glass window on the door, and ineffective door gasket sealing, which are difficult to quantify. The insulation blanket receives heat by conduction from the fins and from the enclosure internal walls and loses heat also by conduction to the external walls of the enclosure. The external walls receive heat by conduction from the insulation blanket and also from the internal walls through the thermal short circuits. Finally, the external walls lose heat by convection and by radiation to the external environment.

The enclosure is divided into six elements: thermosyphons, fins (side walls), enclosure internal walls (back wall, bottom wall, top wall, and door), air, insulation blanket, and external walls. The temperature is assumed to be uniform inside each element. Each element is at a different temperature level, and the elements are thermally connected to each other through radiation, and/or convection and/or conduction heat transfer. Given the complexity of the problem's geometry, an approximate model is developed based on energy balances involving the main heat-transfer modes for each element. The mathematical model of the enclosure consists of a system of ordinary differential equations, obtained through the energy balances. The energy transfer rate coming into the element minus the energy transfer rate coming out of the element must be equal to the rate of accumulation of energy inside the element. Energy comes into and out of the elements in the form of heat (radiation, conduction, convection). Energy is accumulated inside the elements in the form of internal energy, which leads to a rise of the element temperature with time.

Element Energy Balances

In this section, the thermal energy balance for each element is developed.

Thermosyphons

The following thermal energy balance equation is obtained for the thermosyphons:

$$N(m_1 c_{p,i} + m_f c_{v,f})\frac{\partial T_t}{\partial t} = q_e - q_c \tag{1}$$

where c_p (J/kgK) is the specific heat at constant pressure and c_v (J/kgK) is the specific heat at constant volume. The left-hand side of Eq. (1) is related to the thermal inertia of the thermosyphon tube and the working fluid. It is assumed that only the liquid phase contributes to the thermal inertia of the working fluid, that is, the vapor mass is small. The rate of heat transfer from the combustion chamber to the thermosyphon evaporator is q_e (W), while q_c (W) is the rate of heat transfer out of the thermosyphon condenser and into the enclosure. The rate of heat transfer out of the condenser is given by

$$q_c = q_{\text{rad,c-cav}} + q_{\text{cond,c-fin}} + q_{\text{conv,c-air}} \tag{2}$$

The subscripts rad, cond, and conv refer to the mode of heat transfer: radiation, conduction, and convection, respectively. Thus, $q_{\text{rad,c-cav}}$ means the rate of heat transfer by radiation from the condensers of the thermosyphons to the enclosure. Because the thermosyphon condenser surface area is much smaller than the enclosure surface area, the radiation heat transfer between the condenser and the enclosure can be estimated through the following expression:

$$q_{\text{rad,c-cav}} = N(A_c/2)\varepsilon_t \sigma\left(T_t^4 - T_{\text{cav}}^4\right) \tag{3}$$

where ε_t is the emissivity and A_c (m^2) is the area of the condenser external surface. The condenser surface area is divided by two because approximately one-half of the area of the condenser is facing the enclosure. The other half is facing the fin (see Fig. 2). Because the aluminum tape between the thermosyphons and the fin deforms easily under compression to fill the gaps between the two contacting surfaces, there is no exchange of heat by radiation between the thermosyphon and the fin attached to it. The preceding expression is valid for a diffuse, gray, and convex surface of small dimensions inside of a large enclosure at a uniform temperature T_{cav}. In this model, "enclosure" refers to the set of two fins (side walls) and the other internal walls (door, bottom, top, and back walls). Therefore, T_{cav} is not uniform because the fins and internal walls are at different temperatures. The enclosure temperature is defined as

$$T_{\text{cav}}^4 = \left(F_{\text{c-fin}} T_{\text{fin}}^4 + F_{\text{c-i.walls}} T_{\text{i.walls}}^4\right) \Big/ F_{\text{c-cav}} \tag{4}$$

This expression for the enclosure temperature represents a mean value between the temperatures of the fins T_{fin} and of the internal walls $T_{\text{i.walls}}$, weighed by the view factor between the thermosyphon condenser and the fin $F_{\text{c-fin}}$ and the view factor between the condenser and internal walls $F_{\text{c-i.walls}}$. From the rule of the summation of view factors, the view factor between the condenser and enclosure $F_{\text{c-cav}}$ is given by

$$F_{\text{c-cav}} = F_{\text{c-fin}} + F_{\text{c-i.walls}} = 1 \tag{5}$$

The fraction of the radiation energy that the condensers deliver to the fins is calculated as a part of the total radiation that the condensers lose to the enclosure. This fraction is given by the ratio between the view factors from the condenser to the fin $F_{\text{c-fin}}$ and the view factor between the condenser and the enclosure $F_{\text{c-cav}}$, that is,

$$q_{\text{rad,c-fin}} = (F_{\text{c-fin}}/F_{\text{c-cav}}) q_{\text{rad,c-cav}} \tag{6}$$

This fraction is related to the radiation heat transfer between the thermosyphon and the fin on the opposite side of the enclosure. As already mentioned, the radiation heat transfer between the thermosyphon and the fin on the same side of the enclosure is negligible. Despite the approximate nature of Eqs. (3–6), the amount of radiation that the condensers lose to the enclosure is very small and does not affect the overall result, as it will be seen later.

The rate of conduction heat transfer between the thermosyphon condenser and the fins $q_{\text{cond,c-fin}}$ is given by

$$q_{\text{cond,c-fin}} = N[(T_t - T_{\text{fin}})/R_c] \tag{7}$$

The convective heat-transfer rate between the thermosyphon condenser and the air inside the enclosure $q_{\text{conv,c-air}}$ is given by

$$q_{\text{conv,c-ar}} = N h_{\text{int}} \tfrac{2}{3} A_c (T_t - T_{\text{air}}) \tag{8}$$

where h_{int} (W/m^{2}K) is the convection heat-transfer coefficient inside the enclosure. The condenser surface area is multiplied by $\frac{2}{3}$ to account for the part of the condenser area that is in contact with the air, according to Fig. 2.

Fins

For the fins, the following energy balance equation is obtained:

$$m_{\text{fins}} c_{\text{p,fin}} \frac{\partial T_{\text{fins}}}{\partial t} = q_{\text{rad,c-fin}} + q_{\text{cond,c-fin}} - q_{\text{cond,fin-isol}} - q_{\text{cond,fin-i.walls}} - q_{\text{rad,fin-i.walls}} - q_{\text{conv,fin-air}} \tag{9}$$

The fins receive heat from the thermosyphon condensers by radiation $q_{\text{rad,c-fin}}$ and by conduction $q_{\text{cond,c-fin}}$, according to Eqs. (6) and (7). The fins lose heat to the insulation blanket $q_{\text{cond,fin-ins}}$ and the internal walls $q_{\text{cond,fin-i.wall}}$ by conduction, the internal walls $q_{\text{rad,fin-i.wall}}$ by radiation, and the air $q_{\text{conv,fin-air}}$ by convection. These parts are calculated, respectively, through the following equations:

$$q_{\text{cond,fin-ins}} = 2\frac{k_{\text{ins}} A_{\text{fin}}}{e_{\text{ins}}/2}(T_{\text{fin}} - T_{\text{ins}}) \tag{10}$$

$$q_{\text{cond,fin-i.walls}} = 2\frac{T_{\text{fin}} - T_{\text{i.walls}}}{R_{\text{cond,fin-i.walls}}} \tag{11}$$

$$q_{\text{rad,fin-i.walls}} = 2 \times \frac{\sigma\left(T_{\text{fin}}^4 - T_{\text{i.walls}}^4\right)}{[(1-\varepsilon_{\text{fin}})/\varepsilon_{\text{fin}} A_{\text{fin}} + 1/A_{\text{fin}} F_{\text{fin-i.walls}} + (1-\varepsilon_{\text{i.walls}})/\varepsilon_{\text{i.walls}} A_{\text{i.walls}}]} \tag{12}$$

$$q_{\text{conv,fin-air}} = h_{\text{int}} 2 A_{\text{fin}} (T_{\text{fin}} - T_{\text{air}}) \tag{13}$$

The factor two that appears in the numerator of Eq. (10) corresponds to the number of fins, while k_{ins} (W/mK) is the thermal conductivity of the material of the insulation blanket, A_{fin} (m^2) is the surface area of each fin, and T_{ins} (K) is the mean temperature of the insulating blanket. The thermal resistance $R_{\text{cond,fin-i.walls}}$, appearing in Eq. (11), is related to the conduction between the fins and the internal walls through the riveted joints. Equation (12) corresponds to the radiation heat exchange inside an enclosure formed by two gray and diffuse surfaces (fins and internal walls). This expression bears the hypothesis that the thermosyphon condensers do not participate in the radiation heat exchange process between the fins and the internal walls. Put in another way, the amount of radiation emitted by the fins that is reflected by the condensers and reaches the internal walls is very small. This hypothesis is reasonable considering that the dimensions of the thermosyphons are small in comparison with the dimensions of the fins and the internal walls.

Air

The heat balance for the air contained inside the enclosure is

$$m_{\text{air}} c_{\text{p,air}} \frac{\partial T_{\text{air}}}{\partial t} = q_{\text{conv,c-air}} + q_{\text{conv,fin-air}} - q_{\text{conv,air-i.walls}} \tag{14}$$

The air inside the enclosure exchanges heat by convection only, as already mentioned. It receives heat from the condensers and the fins, according to Eqs. (8) and (13) and loses heat to the internal walls $q_{\text{conv,air-i.walls}}$, which is calculated with the following expression:

$$q_{\text{conv,air-i.walls}} = h_{\text{int}} A_{\text{i.walls}} (T_{\text{air}} - T_{\text{i.walls}}) \tag{15}$$

The convective heat-transfer coefficient between the air and the internal walls could be different from the coefficient between the air and the fins, as in Eqs. (8) and (13). However, given the approximate nature of this model, it is reasonable to admit that these coefficients are approximately the same, that is, the local convective heat-transfer coefficient is uniform inside the entire enclosure.

Internal Walls

The following energy balance is adopted for the internal walls:

$$m_{\text{i.walls}}c_{\text{p,i.walls}}\frac{\partial T_{\text{i.walls}}}{\partial t} = q_{\text{rad,c-i.walls}} + q_{\text{rad,fin-i.walls}} + q_{\text{conv,air-i.walls}} + q_{\text{cond,fin-i.walls}} \pm q_{\text{cond,i.walls-ins}} - q_{\text{cond,i.walls-e.walls}} \quad (16)$$

The internal walls receive heat by radiation from the fins [Eq. (12)] and from the thermosyphon condensers, which is estimated through the following expression:

$$q_{\text{rad,c-i.walls}} = (F_{\text{c-i.walls}}/F_{\text{c-cav}})q_{\text{rad,c-cav}} \quad (17)$$

Similarly to Eq. (6), the amount of radiation that the condensers lose to the internal walls is calculated as a fraction of the total radiation that the condensers lose to the entire enclosure. This fraction is given by the ratio between two view factors: condenser to internal walls $F_{\text{c-i.walls}}$ and condenser to enclosure $F_{\text{c-cav}}$. The internal walls also receive heat by convection from the air, according to Eq. (15), and by conduction from the fins through the riveted joints, according to Eq. (11). The internal walls deliver heat by conduction to the insulation blanket $q_{\text{cond,i.walls-ins}}$, which is calculated through the following expression:

$$q_{\text{cond,i.walls-ins}} = \frac{k_{\text{ins}}A_{\text{i.walls}}}{e_{\text{ins}}/2}(T_{\text{i.walls}} - T_{\text{ins}}) \quad (18)$$

The internal walls lose heat directly to the external walls by conduction through thermal short circuits without passing through the insulation blanket. This energy amount, called $q_{\text{cond,i.walls-e.walls}}$, is estimated by means of the following expression:

$$q_{\text{cond,i.walls-e.walls}} = (T_{\text{i.walls}} - T_{\text{e.walls}})/R_{\text{cond,i.walls-e.walls}} \quad (19)$$

where $R_{\text{cond,i.walls-e.walls}}$ is the conduction thermal resistance between the internal and the external walls. This is the short-circuit thermal resistance.

Insulation Blanket

The following heat balance equation is obtained for the insulation blanket:

$$m_{\text{ins}}c_{\text{p,ins}}\frac{\partial T_{\text{ins}}}{\partial t} = q_{\text{cond,i.walls-ins}} + q_{\text{cond,fin-ins}} - q_{\text{cond,ins-e.walls}} \quad (20)$$

The insulation blanket receives heat by conduction from the internal walls $q_{\text{cond,i.walls-ins}}$ [Eq. (18)], and from the fins $q_{\text{cond,fin-ins}}$ [Eq. (10)]. The blanket loses heat by conduction to the external walls $q_{\text{cond,ins-e.walls}}$, which is estimated as

$$q_{\text{cond,ins-e.walls}} = \frac{k_{\text{ins}}A_{\text{e.walls}}}{e_{\text{ins}}/2}(T_{\text{ins}} - T_{\text{e.walls}}) \quad (21)$$

External Walls

The external walls are subjected to the following heat balance equation:

$$m_{\text{e.walls}}c_{\text{p,e.walls}}\frac{\partial T_{\text{e.walls}}}{\partial t} = q_{\text{cond,ins-e.walls}} + q_{\text{cond,i.walls-e.walls}} - q_{\text{conv,e.walls-amb}} - q_{\text{rad,e.walls-amb}} \quad (22)$$

The enclosure external walls receive heat by conduction from the insulation blanket $q_{\text{cond,ins-e.walls}}$ [Eq. (21)] and from the internal walls through the thermal short circuits $q_{\text{cond,i.walls-e.walls}}$ [Eq. (19)]. The external walls lose heat by convection to the external air $q_{\text{conv,e.wall-amb}}$ and by radiation to walls of the external ambient (laboratory) $q_{\text{rad,e.walls-amb}}$. These heat-transfer rates are estimated, respectively, through the following expressions:

$$q_{\text{conv,e.walls-amb}} = h_{\text{ext}}A_{\text{e.walls}}(T_{\text{e.walls}} - T_{\text{amb}}) \quad (23)$$

$$q_{\text{rad,e.walls-amb}} = \varepsilon_{\text{e.walls}}\sigma A_{\text{e.walls}}\left(T_{\text{e.walls}}^4 - T_{\text{amb}}^4\right) \quad (24)$$

Table 1 Geometrical parameters and thermophysical properties of the enclosure

Parameter	Value
A_c, m^2	0.0112
A_{fin}, m^2	0.1344
$A_{\text{i.wall}}$, m^2	1.00
$A_{\text{e.wall}}$, m^2	2.50
$F_{\text{fin-i.wall}}$	0.9
$F_{\text{c-fin}}$	0.08
$F_{\text{c-i.wall}}$	0.92
N	8
m_t, kg	0.135
m_f, kg	0.007
$c_{v,f}$, J/kgK	4000
$c_{p,t}$, J/kgK	440
m_{fin}, kg	1.05
$c_{\text{p,fin}}$, J/kgK	880
ε_{fin}	0.95
ε_t	0.95
$\varepsilon_{\text{i.walls}}$	0.95
$\varepsilon_{\text{e.walls}}$	0.95
m_{ins}, kg	1.3
$c_{\text{p,ins}}$, J/kgK	800
T_{amb}, K	300
m_{air}, kg	0.095
$c_{\text{p,air}}$, J/kgK	1010
$m_{\text{i.walls}}$, kg	5.5
e_{ins}, m	0.035
k_{ins}, m	0.05

In this model, the conduction thermal resistances through the metal sheets were neglected because they are much smaller than the convection resistances between air and these walls. Table 1 presents the values of the geometric parameters and the thermophysical properties that appear in Eqs. (1–24). The thermophysical properties were extracted from the literature[7] at average temperatures between 300 and 650 K, depending on the maximum temperature level reached by each element. The fins are made of commercial aluminum, the internal and external walls are made of mild steel, the thermosyphons are made of stainless steel, the working fluid is water, and the insulation blanket is made of glass wool. The properties are assumed to be constant with the temperature. The view factor between the fin and the internal walls was obtained from the literature.[7] The view factor between the thermosyphon condenser and the fin on the opposite wall was estimated from relations presented by Siegel and Howell.[8] The masses had been measured and the emissivities were estimated from data presented by Incropera and of de Witt[7] for fins and thermosyphons painted black. The internal walls are coated with rough/dark enamel, and the enclosure external walls are white.

The convection heat-transfer coefficient between the external walls and external air was estimated from the correlation of Churchill and Chu for natural convection from a vertical flat surface, as presented by Incropera and de Witt.[7] Under steady-state conditions and at maximum power, the average temperature of the external walls is approximately 70°C. Under these circumstances, the estimated convective heat-transfer coefficient is approximately 5 W/m^{2}K. For the horizontal wall at the top of the enclosure, available correlations in Incropera and de Witt[7] for horizontal plates yield an approximate value of 6 W/m^{2}K. The value of $h_{\text{ext}} = 5$ W/m^{2}K is adopted in the analyses that follow. The internal convective heat-transfer coefficient h_{int} can be estimated from the same correlations of natural convection just mentioned (Incropera and de Witt[7]), and the result is approximately 4 W/m^{2}K. The problem of natural convection inside enclosures is discussed by Incropera and de Witt[7]

and by Bejan,[9] among others. The problem is very complex, and the models presented by these authors refer to boundary conditions where the heat source is located at one of the side walls and the heat sink is located on the opposite wall. Approximate values for the internal heat-transfer coefficient using these correlations are within 3 and 4 W/m^2K. However, these boundary conditions are different from the boundary conditions encountered in the present work, where the enclosure receives heat from the two side walls and loses heat to the walls of the front, back, bottom, and top. An approximate value of $h_{int} = 4\ W/m^2K$ is adopted in the analyses that follow.

At this stage, there are still three unknown parameters to complete the system of equations [Eqs. (1–24)]. They are 1) the thermal resistance between the thermosyphons and the fins R_c, 2) the thermal resistance between the fins and the internal walls $R_{cond,fin\text{-}i.walls}$, and 3) the thermal resistance between the internal and the external walls $R_{cond,i.walls\text{-}e.walls}$ (thermal short circuits).

A brief analysis of the Biot number (Bi) associated to each one of the elements of the enclosure reveals relatively high values of Bi (larger than 1) for the internal walls and the fins in the longitudinal direction. In the direction of the thickness, the values are much smaller than 0.1. Therefore, there is a considerable temperature gradient in the longitudinal direction of the internal walls and the fins. On the other hand, it was assumed in the modeling that these elements were isothermal. Actually, constriction and spreading resistances appear near the interfaces between the metal sheets because the thermal resistance at these interfaces is smaller than the conduction resistance inside the metal sheets. The thermal resistance between the fins and the internal walls $R_{cond,fin\text{-}i.walls}$ takes into account the riveted joint thermal resistance and the constriction and spreading resistances of the fins and of the internal walls. Similarly, the thermal resistance between the internal and the external walls $R_{cond\,i.walls\text{-}e.walls}$ takes into account the riveted joint thermal resistance and the constriction and spreading resistance of the internal walls. The same is valid for the thermal resistance between the thermosyphons and the fins R_c, which is the sum of the joint resistance at the thermosyphon-fin attachment and the spreading resistance of the fin.

All of these thermal resistances are originated at least in part by joint resistances at the contact interface between two elements. When two solids are put into contact, only the highest asperities touch the other surface. Most of the apparent contact area is in fact a gap filled with air. The thermal joint resistance is the association of two thermal resistances in parallel: conduction through the contacting asperities and conduction plus radiation through the gaps. For the problem under study, the gap resistance is much smaller. So, the overall joint resistance is basically the resistance of the gap. Bahrami et al.[10] presents a detailed review of the thermal joint resistance theory. These authors present an analytical model to compute the gap resistance, which depends on rms surface roughness, mean absolute surface slope, contact pressure, Vickers microhardness coefficients, air conductivity, thermal accommodation coefficients caused by the air–solid combination, air mean free path, air Prandtl number, and the ratio of the air specific heats. For the problem under consideration, specific experimental/theoretical studies are necessary in order to model these contact resistances accurately. The main difficulties lie in the flatness deviations of the contacting sheets, their deformation under contact pressure, and the unknown thermo-mechanical properties of the enamel coat. Furthermore, the fins and the internal walls are in essence two-dimensional fins, with spreading resistances presenting complex formulations. Therefore, the resulting model would also be much more complex.

An alternative approach adopted here is to deal with the unknown values of R_c, $R_{cond,fin\text{-}i.walls}$, and $R_{cond,i.walls\text{-}e.walls}$. These thermal resistances are estimated with the help of the model developed in the preceding section. The model, given by the system of equations [Eqs. (1–24)] along with the experimental data of temperature as a function of time,[6] is used in this procedure. It consists of adjusting appropriate values for R_c, $R_{cond,fin\text{-}i.walls}$, and $R_{cond,i.walls\text{-}e.walls}$, so that the predicted temperatures agree with experiments. With the element temperatures adjusted, the radiation, conduction, and convection heat-transfer fractions between the components of the enclosure can be then estimated.

The resulting system of equations [Eqs. (1–24)] is solved numerically using the methodology of finite differences. The time derivatives $\partial T_i/\partial t$ are replaced by $\Delta T_i/\Delta t$, where $\Delta t = 1$ s and ΔT_i is the difference between the temperature of element i at time t and its temperature at time $t - \Delta t$. The system of equations is solved at every time instant t using an implicit formulation scheme with the algebraic manipulation software Maple 8®.

A model similar to the one presented here was developed by da Silva and Mantelli[4] for a bakery oven, where temperature measurements are used as input parameters to the model. The radiation, convection, and conduction heat-transfer fractions are then estimated.

Results and Discussion

In this section, the theoretical model developed in the preceding section is compared against experimental data presented by Milanez

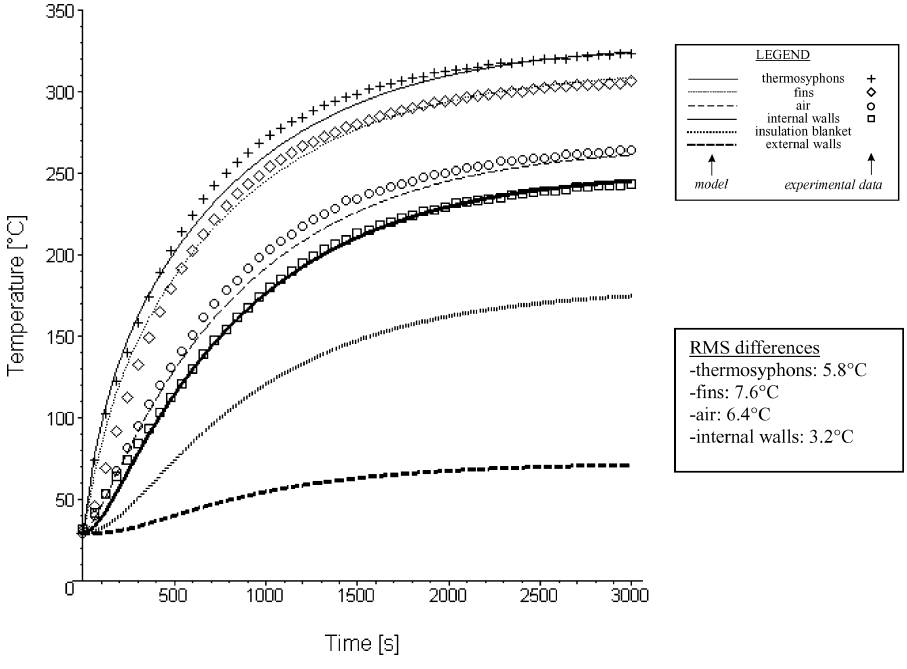

Fig. 3 Comparison between model and experimental data: $R_c = 0.11$ K/W, $R_{cond,fin\text{-}i.walls} = 0.28$ K/W, and $R_{cond,i.walls\text{-}e.walls} = 0.19$ K/W.

and Mantelli.[6] These authors measured the temperature variation with time of a prototype of the enclosure described in this work. The internal walls (back, bottom, and top) were instrumented with seven thermocouples placed in the geometric center and at the border of the each wall. The fins were also instrumented with two thermocouples: one placed 5 mm far from the thermosyphon condenser and the other in the middle of two consecutive thermosyphons. The thermosyphon condensers were instrumented with one thermocouple each, located in the center. The temperature of the air was measured with 27 thermocouples spread inside the enclosure. More details of the experimental setup can be found in Milanez and Mantelli.[6] As discussed before, the fins and the internal walls present relatively large temperature gradients in the longitudinal direction. As a lumped method is employed in the modeling, that is, assuming isothermal elements, the average values of the several thermocouples attached to each element were used in order to compare the measurements with the model.

The thermal resistance of the thermosyphons was experimentally obtained from a thermosyphon isolated from the enclosure. An electrical heater was wrapped around the thermosyphon evaporator, while a fan cooled the condenser. The temperatures at three points of the evaporator and at three points of the condensers were measured by mean of thermocouples. The temperature drop across the thermosyphon was obtained as the difference between the average of the evaporator thermocouples and the average of condenser thermocouples. By dividing the temperature drop by the heat power dissipated in the electrical heater, a value of 0.1 K/W was found in the ranges of temperature and heat-transfer rates of interest. During operation in the enclosure, the average of the temperature drops between the evaporators and the condensers was found to be 16 K. Dividing this value by the thermosyphon total thermal resistance (0.1 K/W), one obtains the average heat-transfer rate through each thermosyphon as 160 W. Multiplying this value by eight, which is the number of thermosyphons, one obtains the total power input as $q_e = 1280$ W, which is the first input to the model.

The next step is to search for values for the three unknown thermal resistances: thermal resistance between thermosyphon and the fins R_c, thermal resistance between the fins and the internal walls $R_{\text{cond,fin-i.walls}}$, and thermal resistance between the internal and external walls $R_{\text{cond,i.walls-e.walls}}$ through the riveted junctions. Figure 3

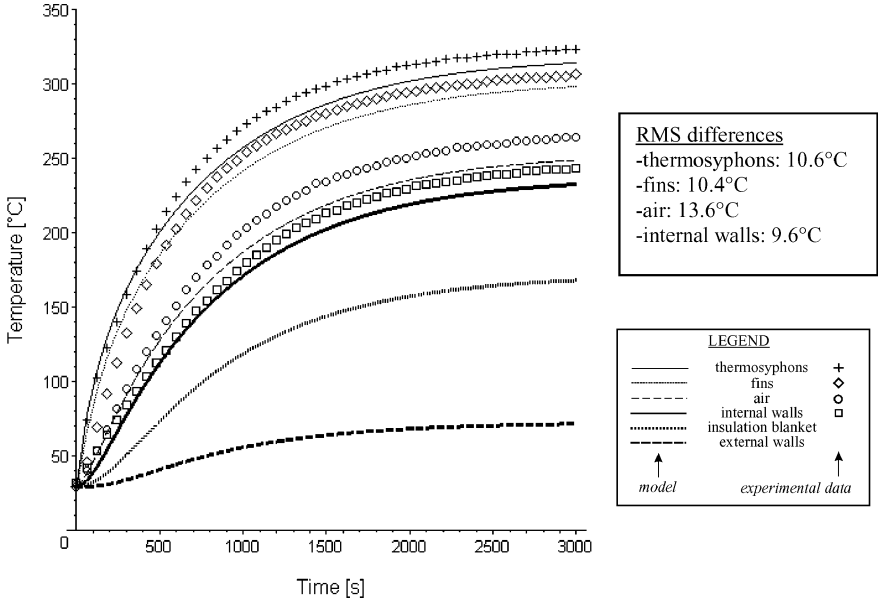

a) $R_{\text{cond,i.walls-e.walls}} = 0.17$ **K/W**

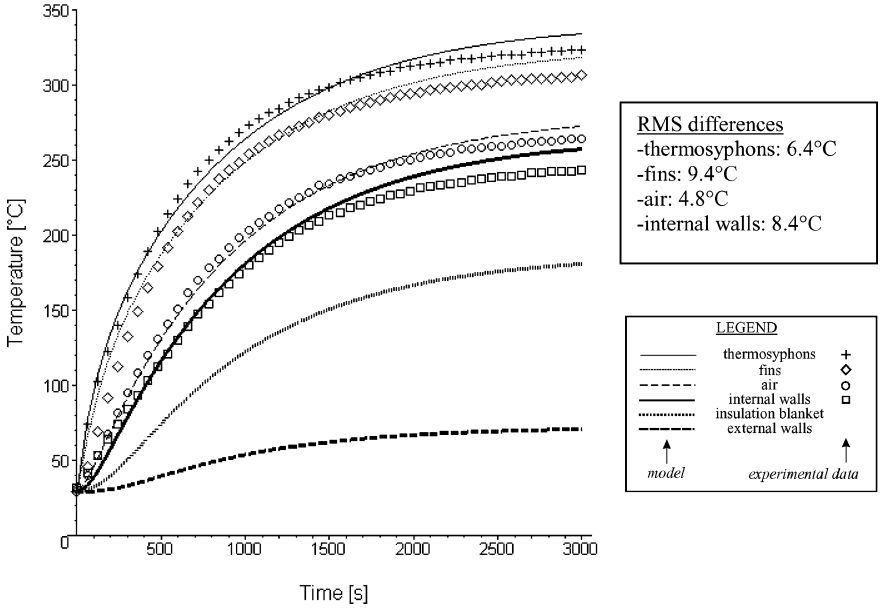

b) $R_{\text{cond,i.walls-e.walls}} = 0.21$ **K/W**

Fig. 4 Parametric analysis of $R_{\text{cond,i.walls-e.walls}}$**.**

shows the temperature measurements as a function of the time collected by Milanez and Mantelli[6] plotted along with the theoretical temperatures computed by the model with $R_c = 0.11$ K/W, $R_{\text{cond,fin-i.walls}} = 0.28$ K/W, and $R_{\text{cond,i.walls-e.walls}} = 0.19$ K/W. These values were obtained by trial and error, so that the theoretical and experimental values of temperature after 3000 s of test are approximately equal. The rms differences between the experiments and the model for each element are also presented in Fig. 3 and vary between 3.4 and 7.6°C. The agreement is fairly good in the entire period of time, given the thermocouple uncertainty of ±1°C and the fact that the thermal properties were assumed constant with temperature in the modeling. The largest differences between the data points and the model curves occur during the early stages of the test (time <500 s), especially for the thermosyphons and the fins. The thermal inertia effects are more intense for time <500 s, especially for the thermosyphons and the fins, which experience a steeper warm-up curve than the other elements. As thermal resistance is generally defined under steady-state conditions, it was opted to adjust the values of R_c, $R_{\text{cond,fin-i.walls}}$, and $R_{\text{cond,i.walls-e.walls}}$ under near steady-state conditions ($t = 3000$ s) rather than to adjust the values so that the rms differences are the smallest possible.

For a given heat power input, the internal wall temperature is practically a function only of the resistance between the internal and external walls $R_{\text{cond,i.walls-e.walls}}$. Therefore, this is the first unknown resistance to be adjusted. Figures 4a and 4b show a parametric study of the temperature curves obtained when values of 0.17 and 0.21 K/W are used in the model, respectively. As one can see, by increasing the value of $R_{\text{cond,i.walls-e.walls}}$ one increases the temperature of the internal walls. Also, the temperature curves of the internal walls, the air, the fins, and the thermosyphons are displaced upwards, but the differences among them remain approximately constant.

Having obtained the first unknown resistance, the next one is the thermal resistance between the fins and the internal walls $R_{\text{cond,fin-i.walls}}$. The fin temperature depends primarily on $R_{\text{cond,fin-i.walls}}$. By matching the fin theoretical temperature to the experimental data, a value of $R_{\text{cond,fin-i.walls}} = 0.28$ K/W was found. Figures 5a and 5b show a parametric study of the temperature curves obtained when values of 0.18 and 0.38 K/W are used, respectively. The larger the value of $R_{\text{cond,fin-i.walls}}$, the higher the temperature of the fins, while the difference between the temperatures of the fins and the thermosyphons remains approximately constant. Finally, the thermal contact resistance between the thermosyphons and the fins is obtained by matching the theoretical and experimental temperatures of the thermosyphons. A value of $R_c = 0.11$ K/W was obtained. Figures 6a and 6b show a parametric study of the temperature

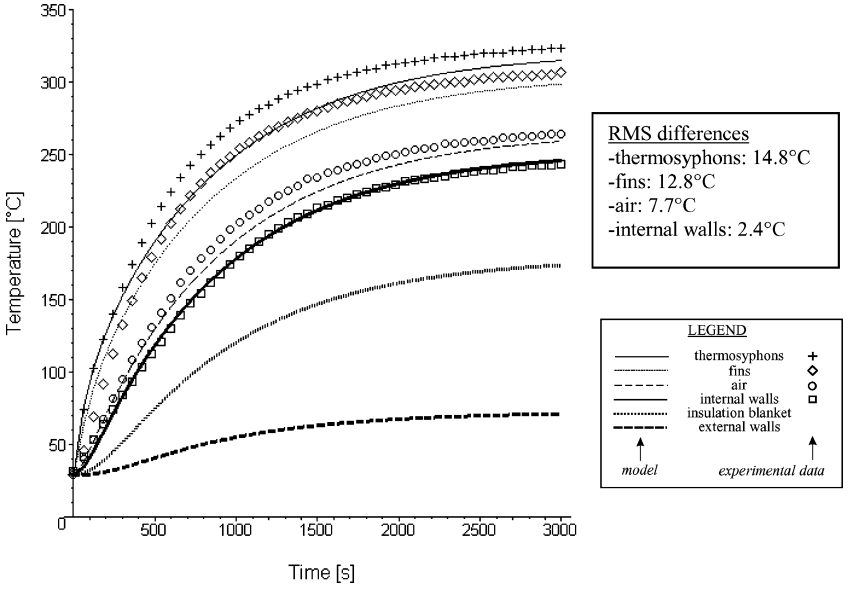

a) $R_{\text{cond,fin-i.walls}}$ = 0.18 K/W

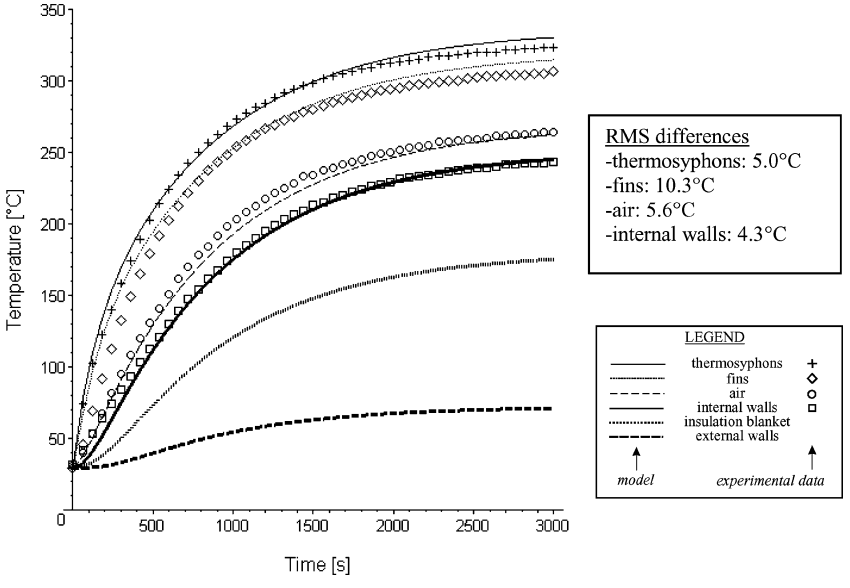

b) $R_{\text{cond,fin-i.walls}}$ = 0.38 K/W

Fig. 5 Parametric analysis of $R_{\text{cond,fin-i.walls}}$.

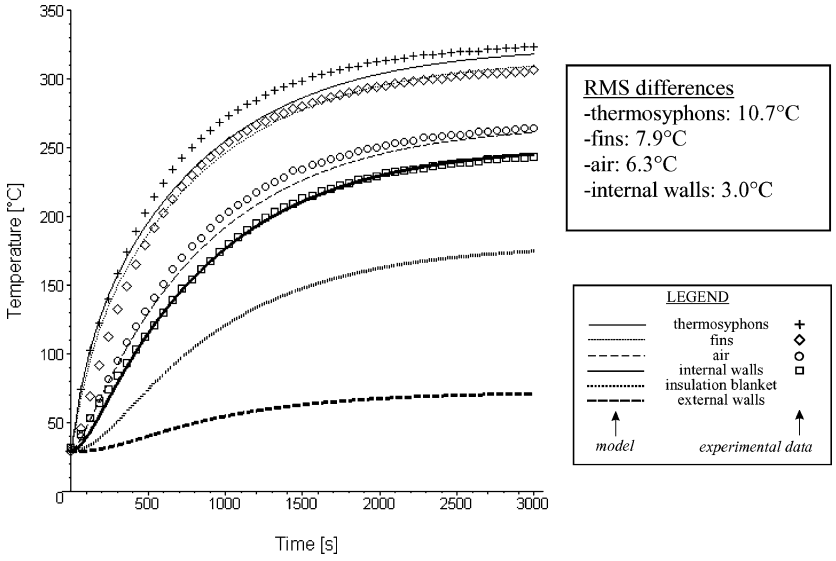

a) R_c **= 0.06 K/W**

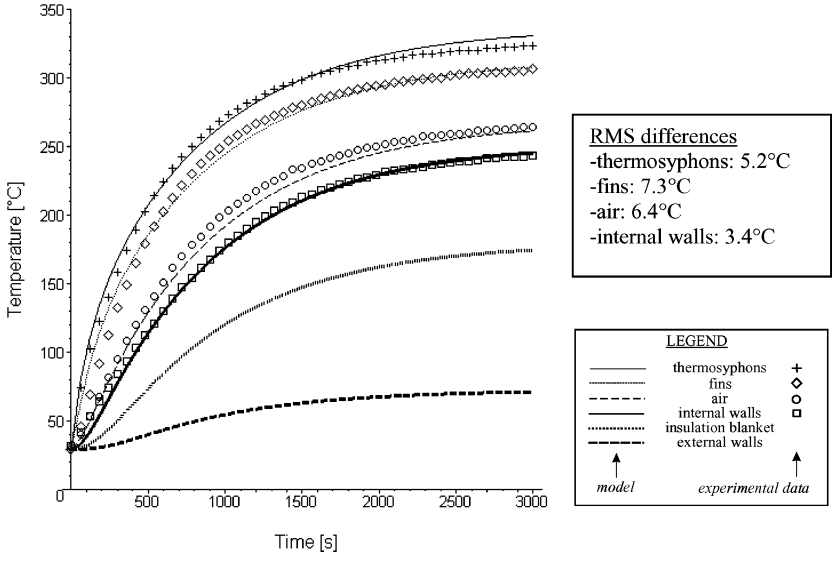

b) R_c **= 0.16 K/W**

Fig. 6 Parametric analysis of R_c.

Table 2 Theoretical and experimental temperatures (°C)

Enclosure element	$t = 1000$ s		$t = 3000$ s	
	Experimental	Theoretical	Experimental	Theoretical
Thermosyphons average	273	273	323	321
Fins	254	257	306	305
Air	200	203	264	257
Internal walls	178	187	243	241
Insulation blanket	——	129	——	173
External walls	——	58	≈70	72

profiles obtained when values of 0.06 and 0.16 K/W are used, respectively. The larger the value of R_c, the higher the temperature of the thermosyphon, while the other temperatures remain approximately constant.

Table 2 shows the measured and the theoretical temperatures after 1000 s and after 3000 s of test. The experimental value of the external wall temperature was measured using an infrared thermometer and represents an approximate average of the external temperature of the enclosure. The unknown thermal resistances were adjusted in order to match the steady-state theoretical temperatures of the internal walls, fins, and thermosyphons to the experimental data (after approximately 3000 s of test). The temperatures of the air, external walls, and insulation blanket are calculated by the model. As one can see, the agreement is good. After 1000 s of test, the theoretical temperatures are slightly higher than the experimental data. These small differences are, at least in part, caused by the thermophysical properties, which were kept constant with temperature.

With the temperatures and the unknown thermal resistances calculated, the radiation, conduction, and convection heat-transfer parcels between the elements of the enclosure can also be calculated. From the total of 1280 W that is transferred into the enclosure by the thermosyphons, 10% is transferred by radiation to the internal walls, and only 1% is transferred by convection to the air. Almost 90% is transferred to the fins by conduction, which shows the importance of the fins in removing the heat from the thermosyphon. This result also shows that the fins are working properly and that the thermal resistance between the fin and the thermosyphons is small.

From the total heat-transfer rate that reaches the fins, 10% is lost to the insulation blanket by conduction, 40% is transferred by conduction to the internal walls through the riveted joints, 46% is transferred by radiation to the internal walls, and only 4% is removed by the air through natural convection. Adding these components with the heat that the air receives directly from the thermosyphons, one observes that only 5% of the enclosure heat input is transferred through the air by convection. This is because the air inside the enclosure is at

Table 3 Percentage of each heat-transfer mode in and out of each element of the enclosure (%)

Enclosure element	Radiation		Convection		Conduction		
	In	Out	In	Out	In	Out	Total
Thermosyphons	——[a]	10	——[a]	1	——[a]	89	100
Fins	1	42	——	4	89	44	90
Air	——	——	5	5	——	——	5
Internal walls	50	——	5	——	35	90	90
Insulation blanket	——	——	——	——	25	25	25
External walls	——	60	——	40	100	——	100

[a]The heat-transfer modes into the thermosyphons in the combustion chamber are not calculated.

Table 4 RMS differences (°C) between model and data as a function of the time-step interval

Enclosure element	$\Delta t = 1$ s	$\Delta t = 2$ s	$\Delta t = 10$ s	$\Delta t = 60$ s
Thermosyphon	5.8	5.8	6.1	8.1
Fin	7.6	7.6	7.4	7.4
Internal walls	6.4	6.4	6.8	9.0
External walls	3.4	3.4	3.3	4.5

a very uniform temperature, as reported by Milanez and Mantelli.[6] These authors observed a maximum temperature difference of only 8°C in the air inside the enclosure. Under these conditions, the air behaves as a thermal insulator. Therefore the heat is removed from the fins mostly by conduction and radiation.

Under steady-state conditions, the thermal insulation blanket transports only 341 W of the total 1280-W power input, which is approximately 25%. If there were no heat leakages, that is, no short circuits between the internal and the external metal sheets that constitute the enclosure, the insulation blanket would transport 100% of the heat input. Therefore, one concludes that the effectiveness of the enclosure insulation is approximately 25%. Approximately 75% is transferred through the thermal short circuits between internal and external walls. It is convenient to mention that the construction approach of the enclosure under study, that is, riveted metal sheets, is commonly used in domestic and industrial ovens. One can then conclude that this approach is not efficient because the thermal insulation is directly related to the fuel consumption. Finally, the external walls of the enclosure lose 60% of the total heat by radiation and 40% by natural convection to the environment. Table 3 presents a summary of the percentages of the heat-transfer modes in and out of each element of the enclosure with respect to the total heat input (1280 W).

Uncertainty Analysis

The thermocouples (K-type) were calibrated in the range of temperatures of interest and presented an uncertainty of ±1°C. The uncertainty of the overall thermal resistance of the thermosyphon is ±7%. The uncertainty of the enclosure heat power input is ±9%.

A study of the influence of the time-step interval value in the numerical solving of the model's equations is summarized in Table 4. It shows the rms differences between data and model for four different values for the time step: 1, 2, 10, and 60 s. As one can see, the difference is very small when one uses either 1, 2, or even 10 s as the time step. As for $\Delta t = 60$ s, the rms differences are larger. Because the computational time is not very sensitive to the time-step interval, $\Delta t = 1$ s is used in this work.

Summary

In this work, a theoretical model is developed in order to analyze the thermal performance of a rectangular enclosure heated by closed two-phase thermosyphons. The enclosure is divided into six main elements. A lumped temperature approach is adopted for each element. The elements are thermally connected among themselves by means of radiation, conduction, and convection heat thermal resistances.

With the input of available experimental data, the model is used to estimate thermal resistances between elements of the enclosure that are difficult to estimate theoretically, such as thermal resistances at riveted joints. The relative importance of the three heat-transfer modes between the elements that constitute the enclosure can also be assessed with the model. The results show that, given the very isothermal characteristic of the air inside the enclosure, which does not lead to effective natural convection heat transfer, most of the heat inside the enclosure is transferred by radiation and conduction. Although radiation and convection are useful in the cooking process, conduction between metal sheets generally means heat leakage and waste of fuel. The results showed that most of the heat transferred into the enclosure is lost through thermal short circuits between the enclosure internal walls and the external environment, without passing through the insulation blanket. This result indicates that the riveted joint approach, generally employed in enclosures such as baking ovens to attach the metal sheets to each other, is thermally inefficient. For example, a thin thermal insulator could be inserted in the riveted joint between the metal sheets, thus increasing the short-circuit resistances $R_{\text{cond,i.walls-e.walls}}$. The model developed here could be used to compare different oven construction techniques. The larger is the value of the thermal resistance between the internal and the external walls, that is, the larger is the short-circuit resistances, the better is the oven thermal insulation. As a consequence, the smaller the startup time is and the smaller the fuel consumption. Also, the impact of new designs on the balance between radiation/convection/conduction, which are very important in the cooking process, can be estimated.

Acknowledgment

The authors would like to acknowledge the support of CENPES-PETROBRÁS during this project.

References

[1]Faghri, A., *Heat Pipe Science and Technology*, Taylor and Francis, Bristol, England, UK, 1995.

[2]Peterson, G. P., *An Introduction to Heat Pipes, Modeling, Testing, and Applications*, Wiley, New York, 1994.

[3]Mantelli, M. B. H., Colle, S., de Carvalho, R. D. M., and de Moraes, D. U. C., "Study of Closed Two-Phase Thermosyphons for Bakery Oven Applications," *Proceedings of the 33rd National Heat Transfer Conference*, American Society of Mechanical Engineers, New York, Aug. 1999, pp. 1–8.

[4]da Silva, A. K., and Mantelli, M. B. H., "Thermal Applicability of Two-Phase Thermosyphons in Enclosures—Experimental and Theoretical Analysis," *Applied Thermal Engineering*, Vol. 24, 2004, pp. 717–733.

[5]Mantelli, M. B. H., Lopes, A., Martins, G. J., Zimmerman, R., Baungartner, R., and Landa, H. G., "Thermosyphon Kit for Conversion of Electrical Bakery Ovens to Gas," *Proceedings of the 7th International Heat Pipe Symposium*, Korean Society of Heat Pipe, Jeju, Korea, 2003, pp. 59–64.

[6]Milanez, F. H., and Mantelli, M. B. H., "A New Methodology for Measuring Heat Transfer Coefficients—Application to Thermosyphon Heated Enclosures," edited by H. Zengqi, S. Xingguo, and Y. Wei, *Proceedings of the 13th International Heat Pipe Conference*, China Astronautics Publishing House, Beijing, 2004, pp. 114–119.

[7]Incropera, F. P., and de Witt, D. P., *Fundamentos de Transferência de Calor e de Massa*, Guanabara Koogan, Rio de Janeiro, 1992, pp. 422–442.

[8]Siegel, R., and Howell, J. R., *Thermal Radiation Heat Transfer*, 3rd ed., Taylor and Francis, Washington, DC, 1992, pp. 1027–1037.

[9]Bejan, A., *Convection Heat Transfer*, 2nd ed., Wiley, New York, 1995, pp. 200–202.

[10]Bahrami, M., Yovanovich, M. M., and Culham, J. R., "Thermal Contact Resistances of Conforming Rough Surfaces with Gas-Filled Gaps," *Journal of Thermophysics and Heat Transfer*, Vol. 18, No. 3, 2004, pp. 318–325.